Kinematic analysis of scissor-like elements using dual quaternions

Juan Gabriel Guerrero Grijalva (juan.guerrero.g@hotmail.com)
Federal University of Santa Catarina https://orcid.org/0000-0001-7593-3110
Edson Roberto De Pieri
Federal University of Santa Catarina

Original Article

Keywords: Mechanisms, kinematics, scissor-like elements, dual quaternion

Posted Date: July 24th, 2020

DOI: https://doi.org/10.21203/rs.3.rs-45973/v1

RESEARCH

Kinematic analysis of scissor-like elements using dual quaternions

Juan Gabriel Guerrero Grijalva[1*] and Edson Roberto De Pieri[1,2]

*Correspondence:
juan.guerrero.g@hotmail.com
[1]Federal University of Santa Catarina, Control and Automation Laboratory, BR 88040-900 Florianopolis, BR
Full list of author information is available at the end of the article

Abstract

This paper presents a standard approach, based on dual quaternions (DQ), to deal with the kinematic analysis of scissor-like elements (SLE). Kinematic relations of homogeneous SLE are simplified by using DQ exponentiation. The steps to identify kinematic singularities are detailed by an algorithm. A second algorithm is introduced to deal with the computation and plotting of reachable and dexterous workspace. In this approach, not just points and vectors, but lines and planes are represented by DQ. The motion of points, lines and planes can be appreciated in practical examples based on domotics.

Keywords: Mechanisms; kinematics; scissor-like elements; dual quaternion

Introduction

The need of making folding equipment ranges from the Mongolian yurts, to more sophisticated devices such as the Da Vinci's umbrella or the velum of the Roman Coliseum [1]. In the last decades, the idea of joining various scissors through a pivot and hinges leaded into more complex assemblies; for example, in 1985 Escrig [2] introduced an approach of translational homogeneous SLEs structures, the next year a novel configuration through polar SLE was presented [3], fourteen years later Hoberman patented a closed structure of symmetrical angulated SLEs [4], leading into the famous toy today known as the Hoberman sphere, the next year Hoberman patented a radial expansion truss structure [5] by using non-symmetrical angulated SLEs. Nowadays, SLEs have been used in aeronautical, architecture, robotics, among other applications [6, 7, 8, 9, 10, 11, 12].

The kinematic analysis of extensive SLE becomes complex because of the large amount of joints and links. Farrugia introduced an approach based on matrices [13] to deal with the kinematics of SLE. The main drawback of this approach is the number of rows and columns in the matrices which depends on the amount of SLEs in the mechanism. The kinematic analysis of SLEs can be developed by using Screw Theory [14]. However, the possibility to deal with the orientation of lines, planes and volumes are not allowed. In [9] it was introduced the use of DQ in the kinematic analysis of translational SLE with constant bar length; nevertheless, the kinematics of connectors was omitted, the application was limited to homogeneous assemblies, and the motion of lines and planes was not explored.

Usually, deployable structures exhibit kinematic singularities along the motion paths [15]. These critical points could lead into the change of mobility [16]. A

robust strategy to control SLE based systems was shown in [17]. This control technique did not consider singularities being possible to lead into collisions that reduce or damage the utility of the mechanism. In this paper, we introduce an algorithm to identify singularities in SLE. If the singularities are detected, then the reachable and dexterous workspace can be computed and plotted by using a second algorithm. Previously, it is necessary to write the kinematic relations of the points of interest from the origin frame. The rotations and translations caused by connectors are considered in this kinematic relations. Extensive homogeneous assemblies of SLE can be simplified by DQ exponentiation being possible to reduce the computational effort [9]. One of the main advantages of DQ is the possibility to orientate lines, planes and volumes [18, 19, 20], we take advantage of this property giving the possibility to include lines and planes, considered as end-effectors, in the kinematic relations of SLE structures.

This document is organized as follows: in the first Section; concepts and terms used in the paper are defined, starting from Clifford algebra, as well propositions to deal with the motion of points, lines and planes in SLE. In the second Section, translational and polar SLE are represented by DQ, connectors employed to assemble three dimensional structures are represented by DQ too. Also, two algorithms to identify singularities and compute the workspace are included in this section. In the third Section; the theory introduced in the first and second Sections is applied in numerical examples based on domotics. Finally, pertinent conclusions and perspectives for future works can be found.

Rigid displacements by Clifford algebra

Quaternions have proven to be efficient at representing rotations with clear geometric meaning [21, 22, 23, 24, 25, 26, 27]; unfortunately, they do not handle translations. Dual quaternions were introduced by William Clifford [28] like an effort to combine rotations and translations while retaining the benefits of the quaternion representation of rotations. In this section, we introduce concepts, notations and definitions about Clifford algebra, as well, its application in the displacement of rigid bodies by dual quaternions. Well known algebraic systems like complex numbers, matrix, vector, quaternion are included in Clifford algebra and unified in a coherent mathematical language [29]. Rotation and translation of geometric entities such points, lines, planes, areas and volumes are basic operations in Clifford algebra, this characteristic will be exploited in the next sections of this paper. We start defining the Clifford algebra.

Definition 1 *A n-dimensional Clifford space (Cl(n)), viewed as an extension of Euclidean vector space, becomes Clifford algebra, with* 2^n *elements, when geometric product is defined. The orthonormal basis* $\{\varsigma_1, \ldots, \varsigma_n\}$ *considered as Euclidean vector* $\mathbb{R}^n$ *is constrained to*

$$\varsigma_i\varsigma_j + \varsigma_j\varsigma_i = 0, \forall i \neq j \quad \wedge \quad \varsigma_i^2 = \varepsilon,$$

where $\varepsilon = \underbrace{+1}_{\lambda^p}, \underbrace{0}_{\lambda^r}, \underbrace{-1}_{\lambda^q}$ *represents the signature of any generator* ς_i.
Aiming for simplicity, the Clifford space is depicted as $Cl_{\lambda^p,\lambda^r,\lambda^q}(n)$. The dimension n of the Clifford space can be computed as the sum of the signatures $\lambda^{p,r,q}$.

Definition 2 *The elements in* $Cl(n)$ *are called according to the amount of generators, i.e, an element with* ς_i *is called vector, with* $\varsigma_i\varsigma_j$ *is called bivector, with* $\varsigma_i\varsigma_j\varsigma_k$ *is called trivector, and so on. The elements with zero generators are scalars.*

Based on Definition 2, a multivector is a general element of Clifford algebra and the number of generators defines the degree of any element.

Definition 3 *A* j*-dimensional subspace of* $Cl(n)$*, defined by homogeneous multivectors of* j *degree, is denoted by* $\langle M\rangle_j$.

By using Definition 3, it is possible to decompose a Clifford space as follows

$$Cl_{\lambda^p,\lambda^r,\lambda^q}(n) = \langle M\rangle_0 \oplus \langle M\rangle_1 \oplus \ldots \oplus \langle M\rangle_n \,. \tag{1}$$

In Eq.(1) " $\oplus$ " represents the direct sum of subspaces.

Definition 4 *The subspaces of* $Cl(n)$ *with even degree, i.e,* $\langle M\rangle_2$, $\langle M\rangle_4$*, and so on, are defined as spinors and the direct sum of the spinors of* $Cl(n)$ *is denoted by* $Cl^+(n)$.

The spinors are employed in rotation and translation of rigid bodies [30, 31, 32], it can be appreciated in the next subsection.

Isomorphism between Clifford algebra and dual quaternions

By using the definitions established above, we introduce the concept of dual quaternion and its property to rotate and translate rigid bodies. The primal Clifford space employed in rigid displacements is $Cl_{0,1,3}(4)$, which belongs to the hyperspace $P\mathbb{R}^3$ with orthonormal basis $\{\varsigma_1^r, \varsigma_1^q, \varsigma_2^q, \varsigma_3^q\}$. Note that by Definition 1 we have

$$(\varsigma_1^r)^2 = 0 \quad \wedge \quad (\varsigma_1^q)^2 = (\varsigma_2^q)^2 = (\varsigma_3^q)^2 = -1.$$

Also, by Definition 1 and 3 note that there exist 2^4 elements in $Cl_{0,1,3}(4)$ as follows

$$\begin{aligned} Cl_{0,1,3}(4) =& \langle M\rangle_0 \oplus \langle M\rangle_1 \oplus \langle M\rangle_2 \oplus \langle M\rangle_3 \oplus \langle M\rangle_4 \\ =& \langle scalar\rangle \oplus \langle \varsigma_1^r, \varsigma_1^q, \varsigma_2^q, \varsigma_3^q\rangle \oplus \langle \varsigma_1^r\varsigma_1^q, \varsigma_1^r\varsigma_2^q, \varsigma_1^r\varsigma_3^q, \varsigma_1^q\varsigma_2^q, \varsigma_2^q\varsigma_3^q, \varsigma_3^q\varsigma_1^q\rangle \\ & \oplus \langle \varsigma_1^r\varsigma_1^q\varsigma_2^q, \varsigma_2^q\varsigma_3^q\varsigma_1^r, \varsigma_3^q\varsigma_1^r\varsigma_2^q, \varsigma_1^q\varsigma_2^q\varsigma_3^q\rangle \oplus \langle \varsigma_1^r\varsigma_1^q\varsigma_2^q\varsigma_3^q\rangle \,. \end{aligned}$$

By Definition 4, the spinors from $Cl_{0,1,3}(4)$ are extracted as follows

$$Cl^+(4) = \langle 1, \varsigma_1^r\varsigma_1^q, \varsigma_1^r\varsigma_2^q, \varsigma_1^r\varsigma_3^q, \varsigma_1^q\varsigma_2^q, \varsigma_2^q\varsigma_3^q, \varsigma_3^q\varsigma_1^q, \varsigma_1^r\varsigma_1^q\varsigma_2^q\varsigma_3^q\rangle \,.$$

Any element h in $Cl^{+}(4)$ can be written as

$$h = 1 + \upsilon_1\varsigma_2^q\varsigma_3^q + \upsilon_2\varsigma_3^q\varsigma_1^q + \upsilon_3\varsigma_1^q\varsigma_2^q + \omega_0\varsigma_1^r\varsigma_1^q\varsigma_2^q\varsigma_3^q + \omega_1\varsigma_1^r\varsigma_1^q + \omega_2\varsigma_1^r\varsigma_2^q + \omega_3\varsigma_1^r\varsigma_3^q.$$

Note that the expression above is formed by one scalar, six bivectors and one tetravector giving a total of eight elements. By Definition 1 the expression above can be rewritten as

$$h = 1 + \upsilon_1\varsigma_2^q\varsigma_3^q + \upsilon_2\varsigma_3^q\varsigma_1^q + \upsilon_3\varsigma_1^q\varsigma_2^q + (\varsigma_1^r\varsigma_1^q\varsigma_2^q\varsigma_3^q)\left[\omega_0 + \omega_1\varsigma_2^q\varsigma_3^q + \omega_2\varsigma_3^q\varsigma_1^q + \omega_3\varsigma_1^q\varsigma_2^q\right]. \tag{2}$$

In Eq.(2) $\upsilon_i, \omega_i \in \mathbb{R}$. If it is used the next relations

$$\varsigma_2^q\varsigma_3^q \leftrightarrow i, \quad \varsigma_3^q\varsigma_1^q \leftrightarrow j, \quad \varsigma_1^q\varsigma_2^q \leftrightarrow k, \quad \varsigma_1^r\varsigma_1^q\varsigma_2^q\varsigma^q \leftrightarrow \varepsilon, \tag{3}$$

then by replacing Eq.(3) in Eq.(2) we have

$$h = 1 + \upsilon_1 i + \upsilon_2 j + \upsilon_3 k + \varepsilon\left[\omega_0 + \omega_1 i + \omega_2 j + \omega_3 k\right]. \tag{4}$$

Definition 5 *A dual quaternion, denoted as* $\mathbb{H}_2$ *, is a dual number composed by eight elements* $\mathbb{H}_2 \in \mathbb{R}^8$*; namely*

$$h = \upsilon_0 + \upsilon_1 i + \upsilon_2 j + \upsilon_3 k + \varepsilon(\omega_0 + \omega_1 i + \omega_2 j + \omega_3 k), \tag{5}$$

where υ_i, ω_i *are real coefficients,* ε *represents the dual unit of the number and* i, j, k *are the unit vector along the* $x-, y-$ *and* $z-$*axes respectively. The elements of* $\mathbb{H}_2$ *satisfy the properties* $i^2 = j^2 = k^2 = ijk = -1$ *and* $\varepsilon^2 = 0$.

From Eq.(4) and Definition 5 we conclude the isomorphism between Clifford algebra and DQ.

Rotation and translation of rigid bodies by dual quaternions

In the Subsection above, starting from the isomorphism with Clifford Algebra, it was detailed the origin of DQ. Here, we use DQ to rotate and translate rigid bodies. Aiming for simplicity, Eq.(5) is represented by

$$h^a = \upsilon^a + \varepsilon\omega^a. \tag{6}$$

Eq.(6) is used in the next definition.

Definition 6 *For two given DQ, h^a and h^b, the homogeneous product is computed as*

$$h^a h^b = \begin{bmatrix} \upsilon_0^a & -\upsilon_1^a & -\upsilon_2^a & -\upsilon_3^a \\ \upsilon_1^a & \upsilon_0^a & -\upsilon_3^a & \upsilon_2^a \\ \upsilon_2^a & \upsilon_3^a & \upsilon_0^a & -\upsilon_1^a \\ \upsilon_3^a & -\upsilon_2^a & \upsilon_1^a & \upsilon_0^a \end{bmatrix} \begin{bmatrix} \upsilon_0^b \\ \upsilon_1^b i \\ \upsilon_2^b j \\ \upsilon_3^b k \end{bmatrix}$$
$$+\varepsilon \left(\begin{bmatrix} \upsilon_0^a & -\upsilon_1^a & -\upsilon_2^a & -\upsilon_3^a \\ \upsilon_1^a & \upsilon_0^a & -\upsilon_3^a & \upsilon_2^a \\ \upsilon_2^a & \upsilon_3^a & \upsilon_0^a & -\upsilon_1^a \\ \upsilon_3^a & -\upsilon_2^a & \upsilon_1^a & \upsilon_0^a \end{bmatrix} \begin{bmatrix} \omega_0^b \\ \omega_1^b i \\ \omega_2^b j \\ \omega_3^b k \end{bmatrix} + \begin{bmatrix} \omega_0^a & -\omega_1^a & -\omega_2^a & -\omega_3^a \\ \omega_1^a & \omega_0^a & -\omega_3^a & \omega_2^a \\ \omega_2^a & \omega_3^a & \omega_0^a & -\omega_1^a \\ \omega_3^a & -\omega_2^a & \omega_1^a & \omega_0^a \end{bmatrix} \begin{bmatrix} \upsilon_0^b \\ \upsilon_1^b i \\ \upsilon_2^b j \\ \upsilon_3^b k \end{bmatrix} \right).$$

It is important to highlight that, in general, the product of DQ does not satisfy the commutative property.

Definition 7 *Two conjugation relations are defined for DQ as follows*

1 Conjugate of DQ: $h^* = \upsilon_0 - \upsilon_1 i - \upsilon_2 j - \upsilon_3 k + \varepsilon(\omega_0 - \omega_1 i - \omega_2 j - \omega_3 k)$.
2 Dual conjugate of DQ: $\bar{h^*} = \upsilon_0 - \upsilon_1 i - \upsilon_2 j - \upsilon_3 k - \varepsilon(\omega_0 - \omega_1 i - \omega_2 j - \omega_3 k)$.

Both DQ conjugations will be used in the motion of points, lines and planes in the propositions introduced in the next subsection.

Definition 8 *A DQ is called unit DQ if $hh^* = 1$. Then, it satisfies the following pair of conditions*

$$\upsilon_0^2 + \upsilon_1^2 + \upsilon_2^2 + \upsilon_3^2 = 1 \quad \wedge \quad \upsilon_0\omega_1 + \upsilon_1\omega_1 + \upsilon_2\omega_2 + \upsilon_3\omega_3 = 0.$$

The conditions detailed in Definition 8 let visualize a unit hypersphere of three dimensions, and a three-dimensional hyperplane perpendicular to the normal at the point $\upsilon_0, \upsilon_1, \upsilon_2, \upsilon_3$ on the hypersphere. Note that the hyperspace $P\mathbb{R}^3 \subset \mathbb{R}^4$, then a DQ representing a rotation and a translation is defined in $\mathbb{R}^8$. This manifold interpretation is used in the next definition.

Definition 9 *Let $\Upsilon = \cos\frac{\vartheta}{2} + \hat{u}\sin\frac{\vartheta}{2}$ be a spinor from $Cl_{0,0,3}(3)$ that represents a rotation about a unit vector $\hat{u}$ through ϑ. Its conjugate is $\Upsilon^* = \cos\frac{\vartheta}{2} - \hat{u}\sin\frac{\vartheta}{2}$ such that $\Upsilon\Upsilon^* = 1$. Let $t = (0, t_x i, t_y j, t_z k)$ be a translation spinor from $Cl_{0,0,3}(3)$. Its corresponding conjugate is $t^* = -t$. A geometric body ξ under the rotation Υ followed by the translation t becomes the point $\Upsilon\xi + t$. The transformation sequence Υ, t can be compacted in the next DQ as follows*

$$\begin{aligned} h =& \Upsilon + \tfrac{\varepsilon}{2} t\Upsilon \\ =& \cos\tfrac{\vartheta}{2} + \hat{u}\sin\tfrac{\vartheta}{2} + \tfrac{\varepsilon}{2}\left(-\sin\tfrac{\vartheta}{2}(t\cdot\hat{u}) + \cos\tfrac{\vartheta}{2} t + \sin\tfrac{\vartheta}{2} t\times\hat{u}\right). \end{aligned}$$

The DQ presented in Definition 9 will be employed in the displacement of points, lines and planes in the next subsection.

Motion of points , lines and planes

The main objective of this paper is to use DQ to analyze the kinematics of SLE assemblies which have a point, a line or a plane such an end-effector. Therefore, in this subsection, by using the definitions depicted in the last subsections, we present the motion of points, lines and planes using DQ.

Proposition 1 *The DQ presented in Definition 9 is a unit DQ.*

Proof. By Definition 8 and 9 we have

$$\begin{aligned} hh^* =&\left(\Upsilon + \tfrac{\varepsilon}{2} t\Upsilon\right)\left(\Upsilon^* + \tfrac{\varepsilon}{2}(t\Upsilon)^*\right) \\ =&\left(\Upsilon + \tfrac{\varepsilon}{2} t\Upsilon\right)\left(\Upsilon^* + \tfrac{\varepsilon}{2}\Upsilon^* t^*\right) \\ =&\Upsilon\Upsilon^* + \tfrac{\varepsilon}{2}\left(\Upsilon\Upsilon^* t^* + t\Upsilon\Upsilon^*\right) \\ =&1 + \tfrac{\varepsilon}{2}\left(t^* + t\right) \\ =&1. \end{aligned}$$

Proposition 2 *For a given point $\mu^p = (0, \mu_x^p i, \mu_y^p j, \mu_z^p k)$ in the hyperspace $P\mathbb{R}^3$, represented in DQ coordinates by $\xi^p = \mathbf{1} + \varepsilon(\mu^p)$, where $\mathbf{1} = (1, 0i, 0j, 0k)$, a rotation Υ and a translation t is represented by ${}'\xi^p = h\xi^p\overline{h^*}$.*

Proof.

$$\begin{aligned} {}'\xi^p =&1 + \varepsilon\left(\Upsilon\xi^p\Upsilon^* + t\right) \\ =&1 + \varepsilon\left(\Upsilon\xi^p\Upsilon^*\right) + \varepsilon t \\ =&1 + \varepsilon\left(\Upsilon\xi^p\Upsilon^*\right) + \varepsilon\tfrac{t}{2} + \varepsilon\tfrac{t}{2} \\ =&1 + \varepsilon\left(\Upsilon\xi^p\Upsilon^*\right) + \varepsilon\tfrac{t}{2} - \varepsilon\tfrac{t^*}{2} \\ =&\left(\Upsilon + \varepsilon\tfrac{t}{2}\Upsilon\right)\left(1 + \varepsilon\xi^p\right)\overline{\left(\Upsilon^* - \varepsilon\Upsilon^*\tfrac{t^*}{2}\right)} \\ =&\left(\Upsilon + \varepsilon\tfrac{t}{2}\Upsilon\right)\left(1 + \varepsilon\xi^p\right)\overline{\left(\Upsilon^* + \varepsilon\Upsilon^*\tfrac{t^*}{2}\right)} \\ =&\left(\Upsilon + \varepsilon\tfrac{t}{2}\Upsilon\right)\left(1 + \varepsilon\xi^p\right)\overline{\left(\Upsilon + \varepsilon\tfrac{t}{2}\Upsilon\right)}^* \\ =&h\xi^p\overline{h^*}. \end{aligned}$$

Proposition 3 *A line in DQ coordinates can be represented by $\xi^L = l + \varepsilon m$, where $l = (0, l_x i, l_y j, l_z k)$ is the vector displacement of the line in the hyperspace $P\mathbb{R}^3$, $m = (0, m')$ with $m' = l \times l_0$ is the moment of the line where l_0 is the position vector of any arbitrary point in the line. Then, a rotation followed by a translation of the line is computed as ${}'\xi^L = h\xi^L h^*$.*

Proof. The rotation in this case affects to the vector displacement $\Upsilon l\Upsilon^*$ as well the moment $\Upsilon m\Upsilon^*$. On the other hand the translation only affects to the moment through $t \times (\Upsilon l\Upsilon^*)$. So, we have

$$\begin{aligned} {}'\xi^L =&\Upsilon l\Upsilon^* + \varepsilon\left[\Upsilon m\Upsilon^* + t \times (\Upsilon l\Upsilon^*)\right] \\ =&\Upsilon l\Upsilon^* + \varepsilon(\Upsilon m\Upsilon^*) + \varepsilon\left[\tfrac{t(\Upsilon l\Upsilon^*) - (\Upsilon l\Upsilon^*)t}{2}\right] \\ =&\Upsilon l\Upsilon^* + \varepsilon(\Upsilon m\Upsilon^*) + \varepsilon\tfrac{t}{2}(\Upsilon l\Upsilon^*) - \varepsilon(\Upsilon l\Upsilon^*)\tfrac{t}{2} \\ =&\left(\Upsilon + \varepsilon\tfrac{t}{2}\Upsilon\right)\left(1 + \varepsilon m\right)\left(\Upsilon^* + \varepsilon\Upsilon^*\tfrac{t^*}{2}\right) \\ =&\left(\Upsilon + \varepsilon\tfrac{t}{2}\Upsilon\right)\left(1 + \varepsilon m\right)\left(\Upsilon + \varepsilon\tfrac{t}{2}\Upsilon\right)^* \\ =&h\xi^L h^*. \end{aligned}$$

Note that the line representation in DQ coordinates is based on *Plücker* coordinates [29, 33].

Proposition 4 *The rotation and translation of a plane, represented in DQ coordinates as* $\xi^N = n - \epsilon d$, *where* $n = (0, n_x i, n_y j, n_z k)$ *is the normal vector represented in the hyperspace* $P\mathbb{R}^3$ *and* $d = (d', 0, 0, 0)$ *where* d' *is the distance of the plane from the origin, is given by* ${}'\xi^N = h\xi^N h^*$.

Proof. The rotation of a plane affects the orientation of the normal vector $\Upsilon n \Upsilon^*$, while the translation affects the distance of the plane from the origin; however, it is necessary to consider the projection of the translation over the normal vector $d + t \cdot (\Upsilon n \Upsilon^*)$. Thus, we have

$$
\begin{aligned}
{}'\xi^N =& \Upsilon n \Upsilon^* - \varepsilon \left[d + t \cdot (\Upsilon n \Upsilon^*) \right] \\
=& \Upsilon n \Upsilon^* - \varepsilon d + \varepsilon \left[\tfrac{t(\Upsilon n \Upsilon^*) + (\Upsilon n \Upsilon^*) t}{2} \right] \\
=& \Upsilon n \Upsilon^* - \varepsilon d + \varepsilon \tfrac{t}{2} (\Upsilon n \Upsilon^*) + \varepsilon (\Upsilon n \Upsilon^*) \tfrac{t}{2} \\
=& \left(\Upsilon + \varepsilon \tfrac{t}{2} \Upsilon \right) (n - \varepsilon d) \overline{\left(\Upsilon^* - \varepsilon \Upsilon^* \tfrac{t^*}{2} \right)} \\
=& \left(\Upsilon + \varepsilon \tfrac{t}{2} \Upsilon \right) (n - \varepsilon d) \overline{\left(\Upsilon^* + \varepsilon \Upsilon^* \tfrac{t^*}{2} \right)} \\
=& \left(\Upsilon + \varepsilon \tfrac{t}{2} \Upsilon \right) (n - \varepsilon d) \overline{\left(\Upsilon + \varepsilon \tfrac{t}{2} \Upsilon \right)}^* \\
=& h \xi^N \overline{h^*}.
\end{aligned}
$$

Note that in Propositions 2, 3 ,and 4 the conjugate of DQ is used in motion of lines and the dual conjugate of DQ is used in points and planes. The definitions and propositions presented in this section are used in the kinematic analysis of SLE structures in the next section.

Kinematic analysis of SLE using DQ

There are translational SLEs with the possibility to translate along a straight trajectory in one ore more axes. Also there are polar SLEs that in addition to translation they have the possibility to rotate through a fixed axis being possible to describe curvilinear trajectories. Moreover, three dimensional folding structures can be assembled by using connectors. In practical application it is possible to find, besides of a point, a line or a plane as end-effector in SLE structures. Thus, by taking advantage of the DQ properties, in this section we introduce an approach to deal with kinematic analysis of complex homogeneous and heterogeneous assemblies of SLEs.

Definition 10 *A SLE unit, also known as pantograph is a composition of two bars connected to each other at an intermediate point through a revolute joint called pivot which allows them to rotate freely about an axis perpendicular to their common plane but constrains all other degrees of freedom. The end points of these bars can be hinged to the next SLE unit, these joints are called hinges depicted on Figure 1. Also, the geometrical parameters of a standard SLE are shown in Figure 1.*

Representation of translational SLE by DQ

There are two types of translational SLEs [34]: the first type with constant bar lengths and the second type with different bar lengths.

Translational SLEs with constant bar lengths: type 1

This type of folding structures can only translate without any rotation. When all bars have the same lengths $a_1 = a_2 = b_2 = b_2 = a_I$, and the pivots are located in the middle of the bars, these assemblies describe an straight translation. Definitions 9 and 10 are employed to describe the kinematic relation of a point in the pivot or the hinges from the origin frame C through a translation spinor $t_I = (0, t_x i, t_y j, 0k)$ as follows.

- From the origin C to the pivot A: $h_{IA} = 1 + \varepsilon t_I$, with $t_x = \frac{\sqrt{4a_I^2 - \delta^2}}{4}$ and $t_y = \frac{\delta}{4}$.
- From the origin C to the upper hinge B_P: $h_{IB_P} = 1 + \varepsilon t_I$, with $t_x = \frac{\sqrt{4a_I^2 - \delta^2}}{2}$ and $t_y = \frac{\delta}{2}$.
- From the origin C to the lower hinge C_P: $h_{IC_P} = 1 + \varepsilon t_I$, with $t_x = \frac{\sqrt{4a_I^2 - \delta^2}}{2}$ and $t_y = 0$.

Note that the input parameters are the SLE aperture δ and the length of the bar a_I. In extensive assemblies of SLEs the most used DQ, among the DQ defined above, is the h_{IC_P}. It happens because the hinge C_P of the i SLE is linked with the hinge C of the $i+1$ SLE, leading into uniform displacement of the origin frame. As seen in the following example.

Example 1 In the SLE structure in Figure 2 the kinematic relation of a point ξ^P in $A_3, A_4, B_{P3}, B_{P4}, C_{P4}$, from the origin C is given by

$$
\begin{aligned}
{}^{A_3}_{C}\xi^P &= h_{IC_P} h_{IC_P} h_{IA} \xi^P \overline{h^*_{IA} h^*_{IC_P} h^*_{IC_P}} \\
{}^{A_4}_{C}\xi^P &= h_{IC_P} h_{IC_P} h_{IC_P} h_{IA} \xi^P \overline{h^*_{IA} h^*_{IC_P} h^*_{IC_P} h^*_{IC_P}} \\
{}^{B_{P3}}_{C}\xi^P &= h_{IC_P} h_{IC_P} h_{IB_P} \xi^P \overline{h^*_{IB_P} h^*_{IC_P} h^*_{IC_P}} \\
{}^{B_{P4}}_{C}\xi^P &= h_{IC_P} h_{IC_P} h_{IC_P} h_{IB_P} \xi^P \overline{h^*_{IB_P} h^*_{IC_P} h^*_{IC_P} h^*_{IC_P}} \\
{}^{C_{P4}}_{C}\xi^P &= h_{IC_P} h_{IC_P} h_{IC_P} h_{IC_P} \xi^P \overline{h^*_{IC_P} h^*_{IC_P} h^*_{IC_P} h^*_{IC_P}}.
\end{aligned}
$$

The relations above come from Proposition 2. Also, it is possible to appreciate that the most used DQ is h_{IC_P} and its dual conjugate. Therefore we consider important to introduce DQ exponentiation for homogeneous DQ in the following point.

DQ exponentiation of translational SLEs: type1 By using Definition 6, if a point $\xi^P = 1 + \varepsilon 0$ is affected by homogeneous motions represented by h_{IC_P} then we can use

$$
\left[{}'\xi^P_I\right]^n = [h_{IC_P}]^n \xi^P \left[\overline{h^*_{IC_P}}\right]^n = [1 + \varepsilon(n\sqrt{4a_I^2 - \delta^2} i + 0j + 0k)],
$$

where n is the number of SLEs. In the Example 1 the relation ${}^{C_{P4}}_{C}\xi^P$ can be rewritten as $[{}^{C_{P4}}_{C}\xi^P_I]^4$, and thus reducing the computational effort [9]. DQ exponentiation can be proven here and in the sequel by using Definition 6 and Proposition 2 as follows

$$
\begin{aligned}
\left[{}'\xi_I^P\right]^1 &= [h_{IC_P}]^1 \xi^P \left[\overline{h^*_{IC_P}}\right]^1 = \quad [1+\varepsilon(\sqrt{4a_I^2-\delta^2}i+0j+0k)]\\
\left[{}'\xi_I^P\right]^2 &= [h_{IC_P}]^2 \xi^P \left[\overline{h^*_{IC_P}}\right]^2 = \quad [1+\varepsilon(2\sqrt{4a_I^2-\delta^2}i+0j+0k)]\\
\left[{}'\xi_I^P\right]^3 &= [h_{IC_P}]^3 \xi^P \left[\overline{h^*_{IC_P}}\right]^3 = \quad [1+\varepsilon(3\sqrt{4a_I^2-\delta^2}i+0j+0k)]\\
&\vdots \qquad\qquad \vdots \qquad\qquad\qquad \vdots\\
\left[{}'\xi_I^P\right]^n &= [h_{IC_P}]^n \xi^P \left[\overline{h^*_{IC_P}}\right]^n = \quad [1+\varepsilon(n\sqrt{4a_I^2-\delta^2}i+0j+0k)].
\end{aligned}
$$

Translational SLEs with different bar lengths: type 2

Similar to the previous case this kind of SLE can only translate without any rotation. Bar lengths are $a_1 = b_2 = a_y$ and $b_1 = a_2 = b_y$. These assemblies describe an inclined translation. Definitions 9 and 10 are used to describe the kinematic relation of a point in the pivot or the hinges from the origin frame C through a translation spinor $t_Y = (0, t_x i, t_y j, 0k)$ as follows.

- From the origin C to the pivot A: $h_{YA} = 1 + \varepsilon t_Y$, with $t_x = \frac{b_Y \cos\tau_Y}{2}$ and $t_y = \frac{b_Y \sin\tau_Y}{2}$ where $\tau_Y = \frac{\pi}{2} - \alpha_Y$; $\alpha_Y = \arccos\left(\frac{\delta^2+b_Y^2-a_Y^2}{2\delta b_Y}\right)$.
- From the origin C to the upper hinge B_P: $h_{YB_P} = 1 + \varepsilon t_Y$, with $t_x = \frac{(a_Y+b_Y)\cos\tau_Y}{2}$ and $t_y = \frac{(a_Y+b_Y)\sin\tau_Y}{2}$; τ_Y, α_Y defined above.
- From the origin C to the lower hinge C_P: $h_{YC_P} = 1 + \varepsilon t_Y$, where $t_x = \frac{b_Y \sin\alpha_Y + a_Y \sin\beta_Y}{2}$ and $t_y = \frac{b_Y \cos\alpha_Y - a_Y \cos\beta_Y}{2}$ with $\beta_Y = \arccos\left(\frac{\delta^2-b_Y^2+a_Y^2}{2\delta a_Y}\right)$; α_Y defined above.

Note that the input parameters are the SLE aperture δ and the lengths of the bars a_Y, b_Y. The DQ presented in this subsection is employed in the next example.

Example 2 In the SLE assembly in Figure 3 the kinematic relation of a point ξ^P inA_3, B_{P2}, C_{P2}, from the origin C is given by

$$
\begin{aligned}
{}^{A_3}_{C}\xi^P &= h_{YC_P} h_{YC_P} h_{YA} \xi^P \overline{h^*_{YA} h^*_{YC_P} h^*_{YC_P}}\\
{}^{B_{P2}}_{C}\xi^P &= h_{YC_P} h_{YB_P} \xi^P \overline{h^*_{YB_P} h^*_{YC_P}}\\
{}^{C_{P2}}_{C}\xi^P &= h_{YC_P} h_{YC_P} \xi^P \overline{h^*_{YC_P} h^*_{YC_P}}.
\end{aligned}
$$

Similar to the last case, DQ exponentiation for this type of SLE is presented in the following point.

DQ exponentiation of translational SLE: type 2 Homogeneous displacements represented by h_{YC_P} in a point $\xi^P = 1 + \varepsilon 0$ can be defined through DQ exponentiation as

$$
\begin{aligned}
\left[{}'\xi_Y^P\right]^n &= [h_{YC_P}]^n \xi^P \left[\overline{h^*_{YC_P}}\right]^n\\
&= [1+\varepsilon(n(b_Y \sin\alpha_Y + a_Y \sin\beta_Y)i + n(b_Y \cos\alpha_Y - a_Y \cos\beta_Y)j + 0k)],
\end{aligned}
$$

where n is the number of SLEs. In the Example 2 the relation ${}^{C_{P2}}_{C}\xi^P$ can be rewritten as $[{}^{C_{P2}}_{C}\xi_Y^P]^2$.

Representation of polar SLEs by DQ

The main characteristic of these structures is to deploy and contract as a part of a single arc. Besides of translation, there exists a rotation by this type of SLE. The lengths of the bars are $a_1 = a_2 = a_S$ and $b_1 = b_2 = b_S$. Definitions 9 and 10 are used to describe the kinematic relation of a point in the pivot or the hinges from the origin frame C through a rotation spinor $\Upsilon_S = \cos\frac{\vartheta}{2} + \hat{u}\sin\frac{\vartheta}{2}$ and a translation spinor $t_S = (0, t_x i, t_y j, 0k)$ as follows.

- From the origin to the pivot A: $h_{SA} = 1 + \varepsilon t_S$, with $t_x = \frac{b_S \cos\tau_S}{2}$ and $t_y = \frac{b_S \sin\tau_S}{2}$ where $\tau_S = \frac{\pi}{2} - \alpha_S; \alpha_S = \arccos\left(\frac{\delta^2 + b_S^2 - a_S^2}{2\delta b_S}\right)$.
- From the origin C to the upper hinge B_P: $h_{SB_P} = 1 + \varepsilon t_S$, with $t_x = \frac{(a_S + b_S)\cos\tau_S}{2}$ and $t_y = \frac{(a_S + b_S)\sin\tau_S}{2}$; τ_S, α_S defined above.
- From the origin C to the lower hinge C_P: $h_{SC_P} = \Upsilon_S + \varepsilon t_S$, where $t_x = \frac{b_S \sin\alpha_S + b_S \sin\beta_S}{2}$ and $t_y = \frac{b_S \cos\beta_S - a_S \cos\alpha_S}{2}$ with $\beta_S = \arccos\left(\frac{\delta^2 - b_S^2 + a_S^2}{2\delta a_S}\right)$; ; $\hat{u} = (0i + 0j + k); \vartheta = -\arctan\left(\frac{(a_S - b_S)\sin\frac{\alpha_S + \beta_S}{2}}{(a_S + b_S)\cos\frac{\alpha_S + \beta_S}{2}}\right)$; α_S defined above.

Note that the input parameters are the SLE aperture δ and the lengths of the bars a_S, b_S. In the next example is applied the DQ presented in this subsection.

Example 3 The kinematic relation of a point ξ^P in the positions A_2, B_{P2}, C_{P3}, in Figure 4 from the origin C is expressed as

$$\begin{aligned}
{}^{A_2}_{C}\xi^P &= h_{SC_P} h_{SA} \xi^P \overline{h^*_{SA} h^*_{SC_P}} \\
{}^{B_{P2}}_{C}\xi^P &= h_{SC_P} h_{SB_P} \xi^P \overline{h^*_{SB_P} h^*_{SC_P}} \\
{}^{C_{P3}}_{C}\xi^P &= h_{SC_P} h_{SC_P} h_{SC_P} \xi^P \overline{h^*_{SC_P} h^*_{SC_P} h^*_{SC_P}}.
\end{aligned}$$

It is important to highlight that the expression above can be employed to displace lines and planes too, being just necessary to replace ξ^L, ξ^N instead of ξ^P. In homogeneous displacements such as ${}^{C_{P3}}_{C}\xi^P$ in the Example 3, based on Definition 6, DQ exponentiation can be used as follows.

DQ exponentiation of polar SLE Homogeneous displacements represented by h_{SC_P} in a point $\xi^P = 1 + \varepsilon 0$ can be defined through DQ exponentiation as

$$\begin{aligned}
\left[{}'\xi^P_S\right]^n &= [h_{SC_P}]^n \xi^P \left[\overline{h^*_{SC_P}}\right]^n \\
&= [1 + \varepsilon(n\left(\sigma_2\sigma_5 - \sigma_1\sigma_6 + \sigma_4\cos\tfrac{\vartheta}{2} - \sigma_3\sin\tfrac{\vartheta}{2}\right) i \\
&\quad + n\left(\sigma_1\sigma_5 + \sigma_2\sigma_6 + \sigma_3\cos\tfrac{\vartheta}{2} + \sigma_4\sin\tfrac{\vartheta}{2}\right) j + 0k)],
\end{aligned}$$

where

$$\begin{aligned}
\sigma_1 &= \tfrac{t_y\cos\frac{\vartheta}{2}}{2} - \tfrac{t_x\sin\frac{\vartheta}{2}}{2}, \quad \sigma_2 = \tfrac{t_x\cos\frac{\vartheta}{2}}{2} + \tfrac{t_y\sin\frac{\vartheta}{2}}{2}, \quad \sigma_3 = \tfrac{\sigma_5 t_y}{2} - \tfrac{\sigma_6 t_x}{2}, \\
\sigma_4 &= \tfrac{\sigma_5 t_x}{2} - \tfrac{\sigma_6 t_y}{2}, \quad \sigma_5 = \cos\tfrac{\vartheta}{2}, \quad \sigma_6 = \sin\tfrac{\vartheta}{2}.
\end{aligned}$$

The parameters t_x and t_y correspond to the DQ h_{SCP}, which relates the lower hinge from the origin. Note that in the Example 3 the expression ${}^{C_{P3}}_{C}\xi^P$ can be replaced by $\left[{}^{C_{P3}}_{C}\xi^P_S)\right]^3$.

Representation of connectors by DQ

The use of connectors in three dimensional SLE structures is quite common. However, the kinematic impact of these connectors generally is small being sometimes ignored or it is considered ideal, it means that the translation that produce these connectors is considered null, i.e, the folding roof presented in [9]. Thereby, aiming for accuracy, in this subsection we introduce a DQ representation of a connector taking into account the rotation and translation that it causes in the assembly. In Figure 5 is depicted a connector with L-shape. The parameters are $\Delta_X, \Delta_Y, \Delta_Z$ that represent translations in $x-, y-, z-$axes respectively, and $\Omega, 0 < \Omega < \pi$ is the angle between the beams of the connector. The above mentioned parameters can be embedded in a DQ through translation and rotation spinors $t_L = (0, \Delta_X, \Delta_Y, -\Delta_Z)$, $\Upsilon_L = \cos\frac{\pi-\Omega}{2} + \hat{u}\sin\frac{\pi-\Omega}{2}$ with $\hat{u} = (0, \pm 1, 0)$. The symbol $\pm$ in $\hat{u}$ is going to depend of the desired rotation according to right-hand rule. Thus, we have $h_L = \Upsilon_L + \frac{\varepsilon}{2} t_L \Upsilon_L$. In Figure 5 is shown a structure composed by two translational SLEs with constant bar (in red), and one polar SLE (in green), both assemblies linked by a connector. Then, the kinematic relation of a point ξ^P in B_P from the origin C is given by

$$ {}^{B_P}_{C}\xi^P = h_{IC_P} h_{IC_P} h_L h_{SB_P} \xi^P \overline{h^*_{SB_P} h^*_L h^*_{IC_P} h^*_{IC_P}}. $$

Analysis of singularities in SLE

Deployable structures, including SLEs, usually deal with singularities. These singularities can cause the change of mobility. Previously to compute the reachable workspace of a folding structure, it is indispensable to identify the singularity points in the path of the mechanism. Thus, in this subsection we introduce Algorithm 1, based on the aforementioned theory, to identify singularities in SLE assemblies.

Algorithm 1 Algorithm for detection of singularities in SLE

procedure PARAMETERS DESCRIPTION
  Define the dimensions of the SLE bars
  Compute $\delta_{MAX} = a_1 + b_1$ ▷ Based on Figure 1
  Determine the kinematic relation ${}^{CP}_{C}\xi$
  Choose the searching increment (S_{bty}) ▷ Searching accuracy
procedure SEARCHING LOOP
  $aux_1 = 100 : -S_{bty} : 0$ ▷ Vector from 100 to 0 with $-S_{bty}$ increment
  $n = size(aux_1)$ ▷ Number of elements in vector aux_1
  $\delta_{[n]} = \delta_{MAX} \times 0.01 \times aux_1$ ▷ Vector with n possible values of δ
  for $i = 1$ **to** n **do**
    ${}^{CP}_{C}\xi_{[i]}(\delta_i)$ ▷ Calculate ${}^{CP}_{C}\xi$ for each interaction
    $t_{[i]} = (0, t_{x[i]}, t_{y[i]}, t_{z[i]})$ ▷ Extract the translation spinor
    if $t_{x[i]}, t_{y[i]}, t_{z[i]} \notin \mathbb{R}$ **then**
      Break ▷ Stop the loop
      $\delta_{BIF} = \delta_{[i]}$ ▷ Value of δ at singularity time

Analysis of workspace in SLE

Analogously to serial robots, SLE structures usually have a end-effector, then it is important to know the dexterous or reachable workspace of SLE mechanisms. The singularity analysis is going to be essential in this point because we can know the limit of the input δ. Therefore, the first step of this approach is to apply Algorithm 1 to compute δ_{BIF}. Some SLE assemblies are free of singularities, if this is the case,

then Algorithm 1 must be omitted. In Algorithm 2 are detailed the steps to calculate and plot the reachable workspace of a SLE structure. If it is desired to compute the dexterous workspace, then in the line 7 of the Algorithm 2 is necessary to replace ℓ by $\ell = 100 \times \delta_{arb}/\delta_{MAX}$ where δ_{arb} is an arbitrary value of $\delta_{arb}, \delta_{MAX} > \delta_{arb} > \delta_{BIF} > 0$.

Algorithm 2 Algorithm for computation and plotting of workspace in SLE

1: **procedure** PARAMETERS DESCRIPTION(Geometry-dimensions)
2: Define the dimensions of the SLE bars
3: Compute $\delta_{MAX} = a_1 + b_1$ ▷ Based on Figure 1
4: Determine the kinematic relation ${}^{CP}_{C}\xi^{P,L,N}$
5: Choose the increment (S_{bty}) ▷ Plotting accuracy
6: **procedure** WORKSPACE COMPUTATION LOOP
7: $aux_1 = 100 : -S_{bty} : \ell$ ▷ Vector from 100 to $\ell = 100 \times \delta_{BIF}/\delta_{MAX}$ with $-S_{bty}$ increment
8: $n = size(aux_1)$ ▷ Number of elements in vector aux_1
9: $\delta_{[n]} = \delta_{MAX} \times 0.01 \times aux_1$ ▷ Vector with n possible values of δ
10: **for** $i = 1$ **to** n **do**
11: ${}^{CP}_{C}\xi_{[i]}(\delta_i)$ ▷ Calculate ${}^{CP}_{C}\xi$ for each interaction
12: $t_{[i]} = (0, t_{x[i]}, t_{y[i]}, t_{z[i]})$ ▷ Extract the translation spinor
13: $\Upsilon_{[i]} = \cos\frac{\vartheta_{[i]}}{2} + \hat{u}\sin\frac{\vartheta_{[i]}}{2}$ ▷ Extract the rotation spinor
14: Plot the orientation of the point, line or plane $\xi^P_{[i]}, \xi^L_{[i]}, \xi^N_{[i]}$

Numerical and practical examples

In this section is applied all the theory presented above in applications based on domotics. The first example is a retractable lamp, the chosen end-effector is a line which emulates the central beam of a light bulb. The second example is a folding furniture for displays like televisions or digital photo frames, which will be represented like a plane. Thus, we can appreciate the DQ advantage of orientate points, lines and planes.

Retractable lamp

The folding structure shown in Figure 6 can be employed to assemble a lamp that could be used over a table, in the corner of a lounge or on the streets to illuminate a public place. The lamp presented below will be used like a hall lamp, and the central beam of light is represented as a line ξ^L. The proposed assembly is presented in Figure 6. The structure is composed by two translational SLEs with constant bar length (in red), two translational SLEs with different bar length (in blue) and three polar SLE (in green). Aiming to plot the reachable workspace, we define the kinematic relations of the points $A_1, B_{P1}, C_{P1}, C_{P2}$ from the origin C.

$$
\begin{aligned}
{}^{A_1}_{C}\xi^P &= h_{IC_P} h_{IC_P} h_{YC_P} h_{YC_P} h_{SC_P} h_{SC_P} h_{SA} \xi^P \overline{h^*_{SA} h^*_{SC_P} h^*_{SC_P} h^*_{YC_P} h^*_{YC_P} h^*_{IC_P} h^*_{IC_P}} \\
{}^{B_{P1}}_{C}\xi^P &= h_{IC_P} h_{IC_P} h_{YC_P} h_{YC_P} h_{SC_P} h_{SC_P} h_{SB_P} \xi^P \overline{h^*_{SB_P} h^*_{SC_P} h^*_{SC_P} h^*_{YC_P} h^*_{YC_P} h^*_{IC_P} h^*_{IC_P}} \\
{}^{C_{P1}}_{C}\xi^P &= h_{IC_P} h_{IC_P} \xi^P \overline{h^*_{IC_P} h^*_{IC_P}} = \left[{}^{C_{P1}}_{C}\xi^P_I \right]^2 \\
{}^{C_{P2}}_{C}\xi^P &= h_{IC_P} h_{IC_P} h_{YC_P} h_{YC_P} \xi^P \overline{h^*_{YC_P} h^*_{YC_P} h^*_{IC_P} h^*_{IC_P}}.
\end{aligned}
$$

The geometric dimensions of the SLE structure in Figure 6 are detailed in Table 1. In Figure 7, by using Algorithm 2, is depicted the reachable workspace of the aforementioned points. In Figure 7 the axes are orientated according to Figure 6.b. In Figure 6.c is highlighted the collision between the bars of the structure, when

$\delta = \delta_{BIF}$, leading into the lost of mobility. By using the numerical values shown in Table 1 and the Algorithm 1 we compute $\delta_{BIF} = 0.19$ m, it means that the reachable workspace is computed for $0.5 > \delta > 0.19$ m. The kinematic relation for the line ξ^L depicted in Figure 6.b. is defined as follows

$$\overset{A_1}{C}\xi^L = h_{IC_P}h_{IC_P}h_{YC_P}h_{YC_P}h_{SC_P}h_{SC_P}h_{SA}\xi^L h^*_{SA}h^*_{SC_P}h^*_{SC_P}h^*_{YC_P}h^*_{YC_P}h^*_{IC_P}h^*_{IC_P}.$$

In the expression above, the line ξ^L has a vector displacement $l^{'} = (1.5i, 0j, 0k)$ and a moment $m^{'} = 0$. Because of Proposition 2, note that the kinematic relation above employs conjugation of DQ instead of dual conjugation of DQ. By using $\overset{A_1}{C}\xi^L$, in Figure 8 is plotted the lines orientation for $\delta = 0.202, 0.23, 0.29, 0.36, 0.45, 0.5$. Now we interpret a numerical example, for $\delta = 0.45$ m the value of $\overset{A_1}{C}\xi^L$ is

$$\overset{A_1}{C}\xi^L = [0 + 1.37i - 0.62j + 0k + \varepsilon(0 + 0i + 0j - 0.4461k)]. \tag{7}$$

From Eq.(7), we extract the displacement vector $l^{'} = (1.37i - 0.62j + 0k)$ and the moment $m^{'} = (0i + 0j - 0.4461k)$ by using $l_0 = l^{'} \times m^{\cdot}$ we compute $l_0 = (0.2765i + 0.6094j + 0k)$ being any arbitrary point over the line. If it is desired to orientate the line segment as depicted in Figure 8, then we can use $l^{'} = P_F - P_S$ where P_F is the final point and P_S is the starting point of any segment line. Thus, by using $\overset{A_1}{C}\xi^P$, the starting point can be extracted, then the value of $l^{'}$ can be extracted from $\overset{A_1}{C}\xi^L$.

Folding furniture for displays

Each year the size of televisions increases while the area of the rooms decreases. One possible solution to this contradiction is to fix the display on the wall. The main drawback is that the display can not be inclined. The furniture presented in this subsection was designed to be fixed on the roof of a room (see figure 9.a), moreover offers the possibility to regulate the inclination. Then, in this example we intend to apply the orientation of planes emulating flat displays, as well the use of connector to create a three dimensional structure. The structure is composed by one translational SLE with constant bar length (in red), one connector (see Figure 9.b), one translational SLE with different bar length (in blue), and two polar SLEs (in green). The kinematic relations of the points A_1, C_{P1}, C_{P2} from the origin frame C can be written as follows

$$\begin{aligned}
\overset{A_1}{C}\xi^P &= h_{IC_P}h_L h_{YC_P}h_{SC_P}h_{SA}\xi^P \overline{h^*_{SA}h^*_{SC_P}h^*_{YC_P}h^*_L h^*_{IC_P}} \\
\overset{C_{P1}}{C}\xi^P &= h_{IC_P}\xi^P \overline{h^*_{IC_P}} \\
\overset{C_{P2}}{C}\xi^P &= h_{IC_P}h_L h_{YC_P}\xi^P \overline{h^*_{YC_P}h^*_L h^*_{IC_P}}.
\end{aligned} \tag{8}$$

The connector h_L in Eq.(8) has $\Omega = \pi/2$ and $\Delta_X = 0.5, \Delta_Z = -1$ cm according to Figure 5. By using Algorithm 1 the value of δ at singularity time was computed as $\delta_{BIF} = 0.2$ m. This time the singularity was caused by a jam as depicted in Figure 9.b. The dimensions of the bars are the same depicted in Table 1. In Figure 10, by using Algorithm 2, it is plotted the reachable workspace of the arbitrary chosen points A_1, C_{P1}, C_{P2} in Figure 9.b. Because of the connector Figure 10, becomes

three dimensional. Now, we assume that there is a television display fixed in the point A_1. Based on Proposition 4 the plane of the display can be represented by $\xi^N = n - \varepsilon d$, where $n = (0, i, 0j, 0k)$ and $d = 0$ at the origin. The kinematic relation of the plane from the origin is given by

$$ {}^{A_1}_{C}\xi^N = h_{IC_P} h_L h_{YC_P} h_{SC_P} h_{SA} \xi^N \overline{h^*_{SA} h^*_{SC_P} h^*_{YC_P} h^*_L h^*_{IC_P}}. \tag{9} $$

Note that in Eq.(9) is employed the dual conjugation according to Proposition 4. In Figure 11, the orientation of planes are plotted according to various values given to δ. Now, we interpret one of the plotted result, in the case of $\delta = 0.43$ m the orientation of the plane was

$$ {}^{A_1}_{C}\xi^N = \left[0 + 0i - 0.26j - 0.97k - \varepsilon\left(0.48 + 0i + 0j + 0k\right)\right], $$

which means a plane with normal vector $n = (0i - 0.26j - 0.97k)$ at distance $d = 0.48$ m from the origin. However, if it is desired to compute a point in the plane, then we can use ${}^{A_1}_{C}\xi^P$ from Eq.(8). Through the development of the numerical examples shown in this section, we applied all the theory introduced above, based on these results and other experiences acquired throughout this research in the next section we detail the main conclusions and possible future work.

Conclusions and future work

This paper addresses the kinematic analysis of SLE structures based on DQ. It starts from the representation of SLE, connectors, and end-effectors by DQ. Kinematic relations of homogeneous assemblies of SLEs are simplified by using DQ exponentiation. The analysis of singularities is developed by Algorithm 1. If there exist singularities in the SLE structure, then , by using Algorithm 2, they are considered in the computation and plotting of reachable or dexterous workspace. In the practical examples, the theory developed along the paper was applied. Also, it was possible to appreciate the dual quaternions characteristics to orientate points, lines and planes.

In future works, we intend to present a complete analysis and interpretation of singularities in SLE; thereby, control strategies to deal with these singularities. Also, we perceived that this approach can be applied to serial and parallel mechanisms or robots, by using the same concept, it means to represent mechanical elements by DQ, then the kinematic relation can be written in the same way presented in this paper. Differential kinematics based on DQ is expected to be explored being possible to define conditions and theorems to deal with the kinematic control of SLEs.

Declaration

Availability of data and materials

Data sharing is not applicable to this article as no datasets were generated or analysed during the current study.

Competing interests

The authors declare that they have no competing interests.

Funding

This paper had the financial support of the Brazilian funding agency CAPES (Grant n.40410) during its study and writing.

Author's contributions

ERP described the mathematical approach related to Clifford algebra as well its relation with dual quaternions, and the use of them in the positioning of points, lines and planes as end-effectors in SLEs. JGGG programmed and simulated the use of dual quaternions in SLEs, and was a major contributor in writing the manuscript. Both authors read and approved the final manuscript.

Acknowledgements

We would like to gratefully acknowledge the support of the CTC-UFSC for let us use the Control and Automation Laboratory during this research.

Author details

[1]Federal University of Santa Catarina, Control and Automation Laboratory, BR 88040-900 Florianopolis, BR.
[2]Department of Mechanical Engineering, Raul Guenther Robotics Laboratory, BR 88040-900 Florianopolis, BR.

References

1. De Temmerman, N.: Design and analysis of deployable bar structures for mobile architectural applications. Vrije Universiteit Brussel (2007)
2. Escrig, F.: Expandable space structures. International Journal of Space Structures **1**(2), 79–91 (1985)
3. Zanardo, A.: Two-dimensional articulated systems developable on a single or double curvature surface. Meccanica **21**(2), 106–111 (1986)
4. Hoberman, C.: Reversibly expandable doubly-curved truss structure. Google Patents. US Patent 4,942,700 (1990)
5. Hoberman, C.: Radial expansion/retraction truss structures. Google Patents. US Patent 5,024,031 (1991)
6. Thomson, M.W., Lisman, P.D., Helms, R., Walkemeyer, P., Kissil, A., Polanco, O., Lee, S.-C.: Starshade design for occulter based exoplanet missions. In: Space Telescopes and Instrumentation 2010: Optical, Infrared, and Millimeter Wave, vol. 7731, p. 773153 (2010). International Society for Optics and Photonics
7. Zhao, J.-S., Wang, J.-Y., Chu, F., Feng, Z.-J., Dai, J.S.: Mechanism synthesis of a foldable stair. Journal of Mechanisms and Robotics **4**(1) (2012)
8. Gonzalez, D.J., Asada, H.H.: Design and analysis of 6-dof triple scissor extender robots with applications in aircraft assembly. IEEE Robotics and Automation Letters **2**(3), 1420–1427 (2017)
9. Grijalva, J.G., De Pieri, E.R., Martins, D.: Dual-quaternion on simple scissor-like elements. In: IFToMM World Congress on Mechanism and Machine Science, pp. 449–458 (2019). Springer
10. Yang, Y., Peng, Y., Pu, H., Chen, H., Ding, X., Chirikjian, G.S., Lyu, S.: Deployable parallel lower-mobility manipulators with scissor-like elements. Mechanism and Machine Theory **135**, 226–250 (2019)
11. Zhao, N., Luo, Y., Deng, H., Shen, Y.: The deformable quad-rotor: Mechanism design, kinematics, and dynamics effects investigation. Journal of Mechanisms and Robotics **10**(4) (2018)
12. Xu, Y., Chen, Y., Liu, W., Ma, X., Yao, J., Zhao, Y.: Degree of freedom and dynamic analysis of the multi-loop coupled passive-input overconstrained deployable tetrahedral mechanisms for truss antennas. Journal of Mechanisms and Robotics **12**(1) (2020)
13. Farrugia, P.: Kinematic analysis of foldable structures. PhD Thesis, University of Surrey, United Kingdom (2008)
14. Zhao, J.-S., Chu, F., Feng, Z.-J.: The mechanism theory and application of deployable structures based on sle. Mechanism and Machine Theory **44**(2), 324–335 (2009)
15. Chen, Y., Feng, J., Liu, Y.: A group-theoretic approach to the mobility and kinematic of symmetric over-constrained structures. Mechanism and Machine Theory **105**, 91–107 (2016)
16. Qin, Y., Dai, J.S., Gogu, G.: Multi-furcation in a derivative queer-square mechanism. Mechanism and machine theory **81**, 36–53 (2014)
17. Grijalva, J.G., De Pieri, E.R., Martins, D.: Robust control of scissor-like elements based systems. Mechanism and Machine Theory **150**, 103849 (2020)
18. Chevallier, D.: Lie algebras, modules, dual quaternions and algebraic methods in kinematics. Mechanism and Machine Theory **26**(6), 613–627 (1991)
19. Radavelli, L.A., De Pieri, E.R., Martins, D., Simoni, R.: Points, lines, screws and planes in dual quaternions kinematics. In: Advances in Robot Kinematics, pp. 285–293. Springer, (2014)
20. Liu, K., Kong, X., Yu, J.: Operation mode analysis of lower-mobility parallel mechanisms based on dual quaternions. Mechanism and Machine Theory **142**, 103577 (2019)
21. Tsai, L. W.: Robot Analysis: the Mechanics of Serial and Parallel Manipulators. John Wiley & Sons, (1999)
22. Dai, J.S.: Euler–rodrigues formula variations, quaternion conjugation and intrinsic connections. Mechanism and Machine Theory **92**, 144–152 (2015)
23. Benciolini, B., Vitti, A.: A new quaternion based kinematic model for the operation and the identification of an articulated arm coordinate measuring machine inspired by the geodetic methodology. Mechanism and Machine Theory **112**, 192–204 (2017)
24. Yu, J., Jin, Z., Kong, X.: Identification and comparison for continuous motion characteristics of three two-degree-of-freedom pointing mechanisms. Journal of Mechanisms and Robotics **9**(5) (2017)
25. Jianguo, C., Yangqing, L., Ruijun, M., Jian, F., Ya, Z.: Nonrigidly foldability analysis of kresling cylindrical origami. Journal of Mechanisms and Robotics **9**(4) (2017)
26. Li, J., Michael McCarthy, J.: Analysis of two spherical parallel manipulators with hidden revolute joints. Journal of Mechanisms and Robotics **9**(3) (2017)
27. Li, X., Ge, X., Purwar, A., Ge, Q.: A unified algorithm for analysis and simulation of planar four-bar motions defined with r-and p-joints. Journal of Mechanisms and Robotics **7**(1) (2015)
28. Clifford, W.K.: Preliminary sketch of bi-quaternions. Proceedings of the London Mathematical Society **s1–4(1)**, 381–395 (1873)

29. Radavelli, L., Simoni, R., De Pieri, E., Martins, D.: A comparative study of the kinematics of robots manipulators by denavit-hartenberg and dual quaternion. Mecánica Computacional, Multi-Body Systems **31**(15), 2833–2848 (2012)
30. Hestenes, D.: New Foundations for Classical Mechanics vol. 15. Springer, (2012)
31. Lounesto, P.: Clifford Algebras and Spinors vol. 286. Cambridge university press, (2001)
32. Selig, J.M.: Geometric Fundamentals of Robotics. Springer, (2004)
33. Featherstone, R.: Plucker basis vectors. In: Proceedings 2006 IEEE International Conference on Robotics and Automation, 2006. ICRA 2006., pp. 1892–1897 (2006). IEEE
34. Akgün, Y.: A novel transformation model for deployable scissor-hinge structures. PhD Thesis, Universitat Stuttgart, Stuttgart (2010)

Figures

Figure 1 Scissor-like element. Parts of standard SLE and its geometrical parameters.

Figure 2 Folding structure. Composed by four translational SLEs with constant bar lenght.

Figure 3 Folding structure. Composed by three translational SLEs with different bar lenght.

Figure 4 Folding structure. Composed by three polar SLEs.

Figure 5 Connector. Description of its geometrical parameters.

Figure 6 Retractable lamp. a. folding state b. intermediate position c. collision.

Figure 7 Workspace analysis. Reachable workspace of points $A_1, B_{P1}, C_{P1}, C_{P2}$.

Figure 8 Light beam. Orientation of the light beam represented by a line on the x-y frame.

Figure 9 Folding furniture for flat displays. a. deploying condition b. singularity c. side view d. front view.

Figure 10 Workspace analysis. Reachable workspace: points A_1, C_{P1}, C_{P2}.

Tables

Figure 11 Folding furniture for TV. Orientation for planes emulating a flat display.

Table 1 Bar length dimensions of Figures 6 and 9.

	a_I	a_Y	b_Y	a_S	b_S
Bar length [meters]	0.25	0.3	0.2	0.35	0.15

Figures

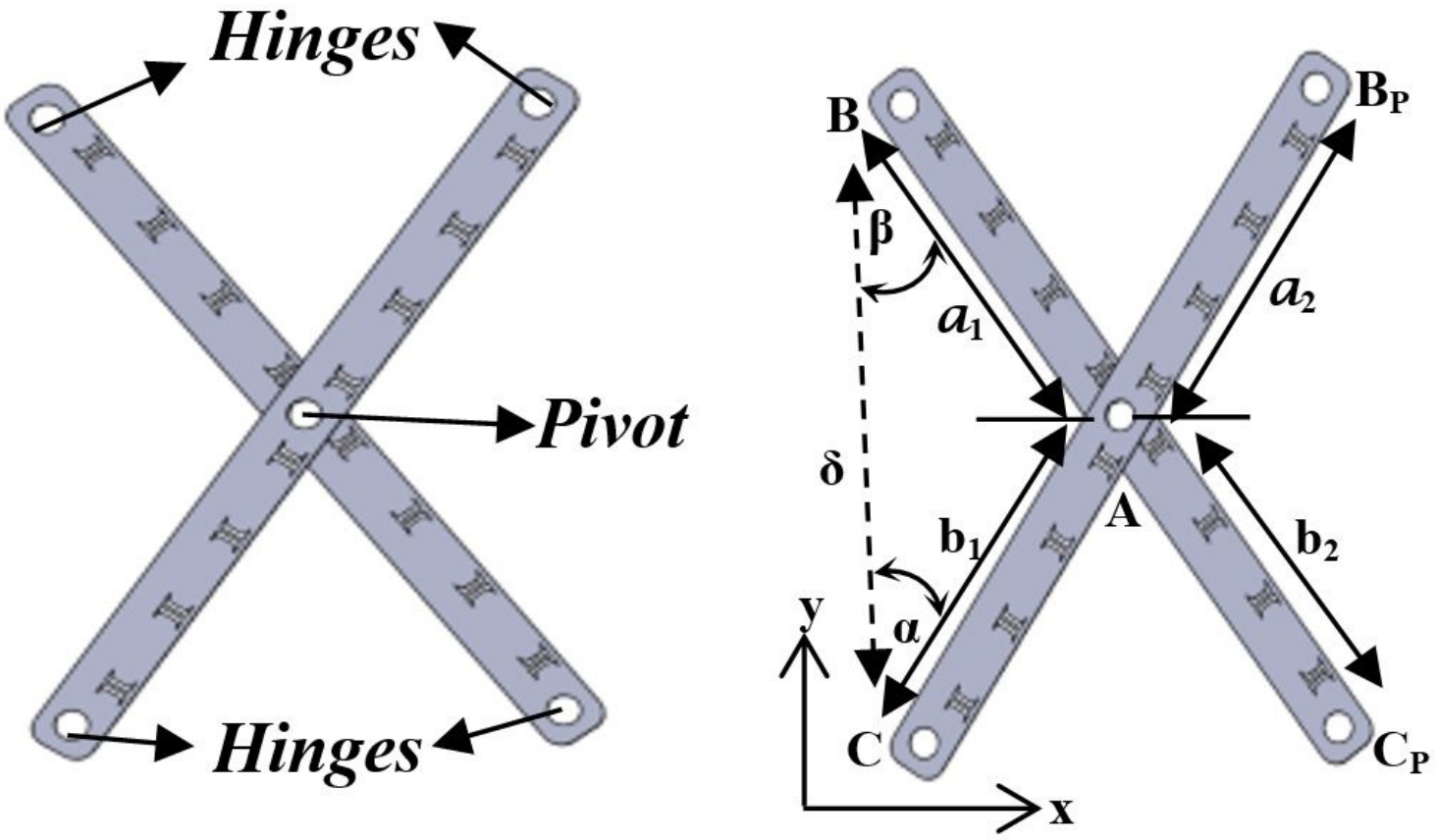

Figure 1

Scissor-like element. Parts of standard SLE and its geometrical parameters.

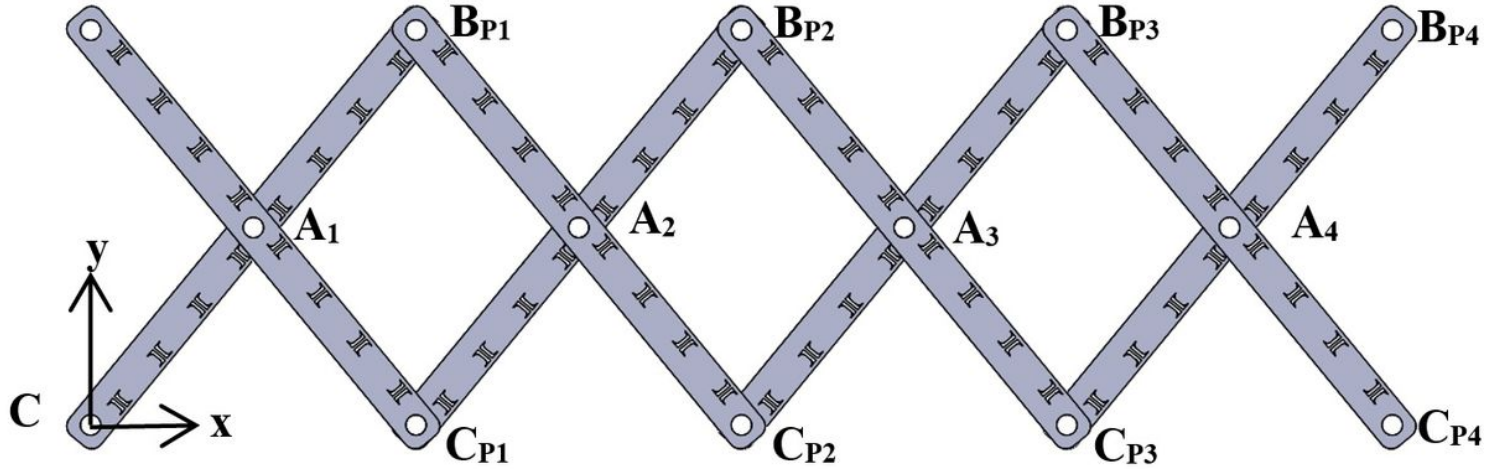

Figure 2

Folding structure. Composed by four translational SLEs with constant bar length.

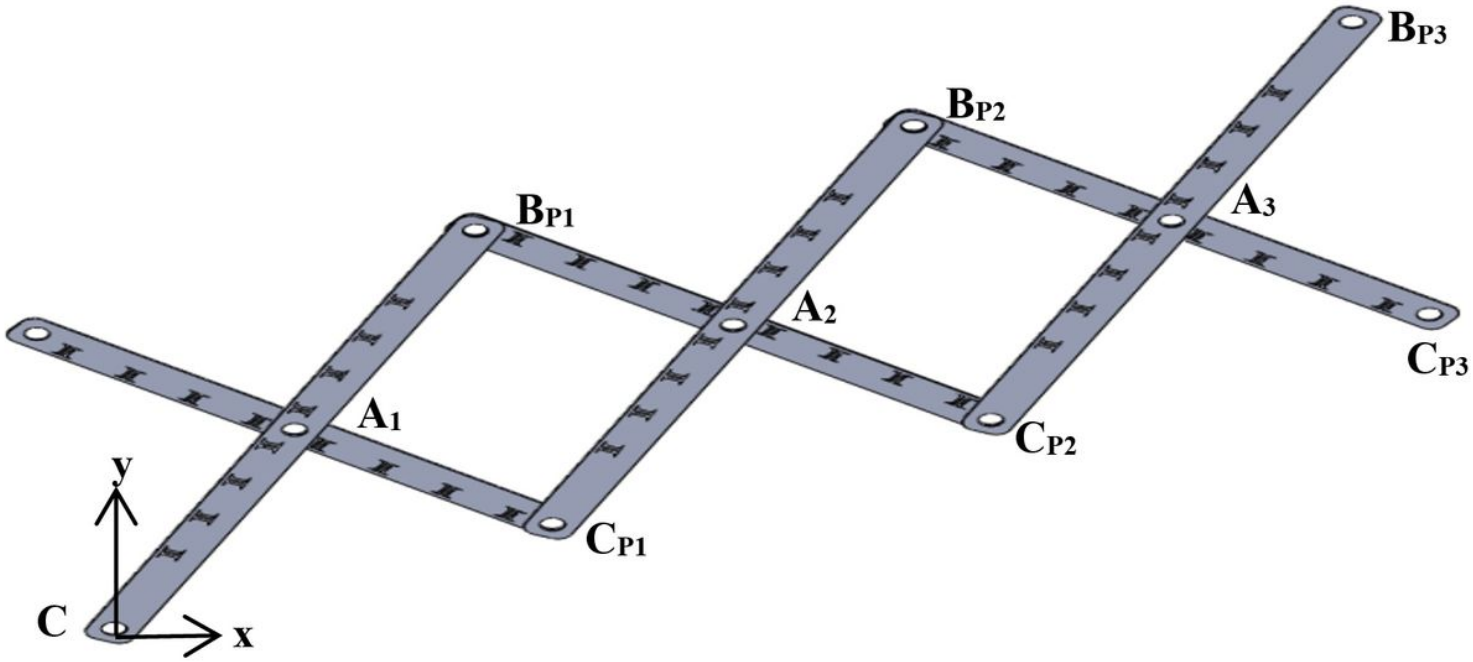

Figure 3

Folding structure. Composed by three translational SLEs with different bar length.

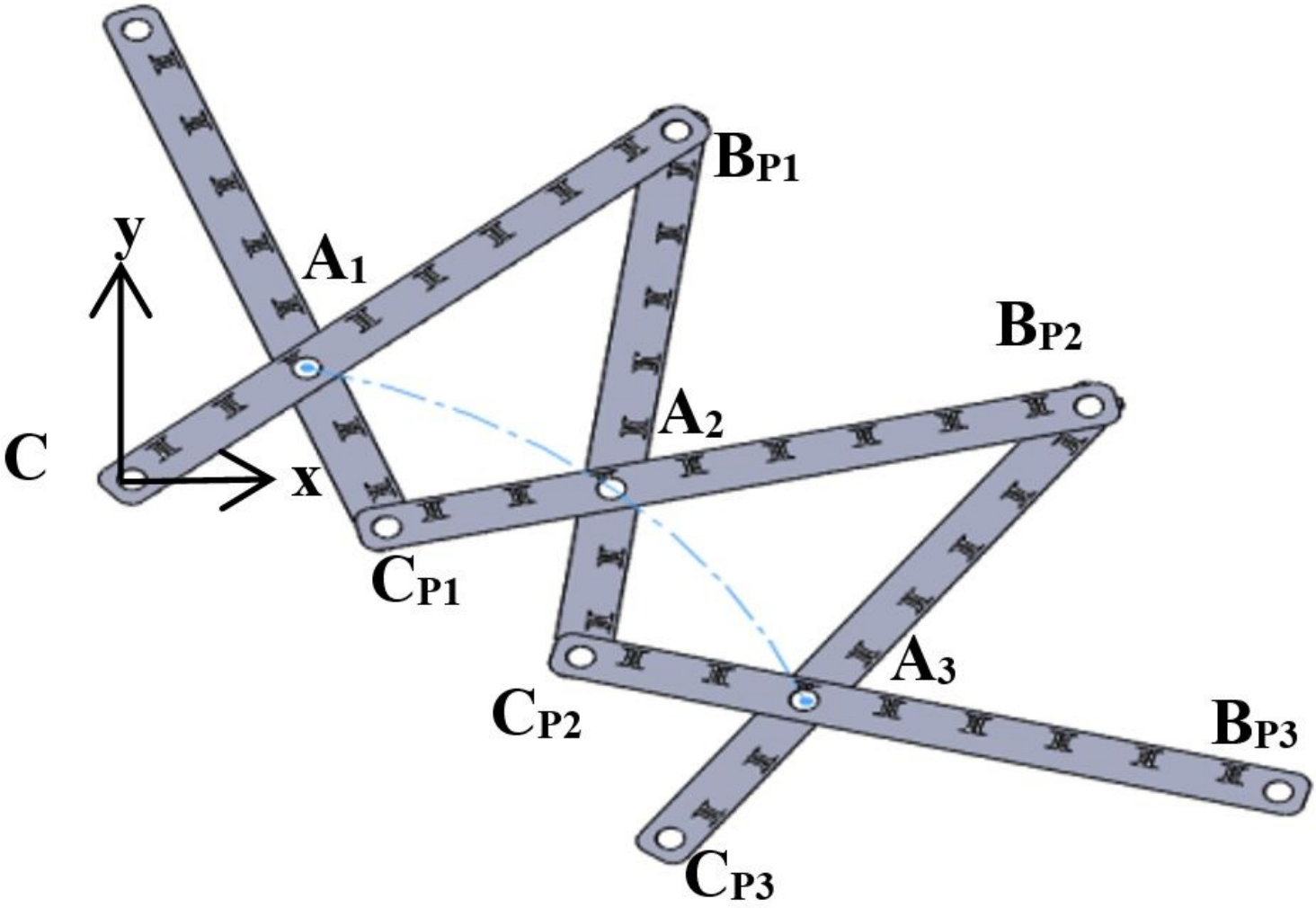

Figure 4

Folding structure. Composed by three polar SLEs.

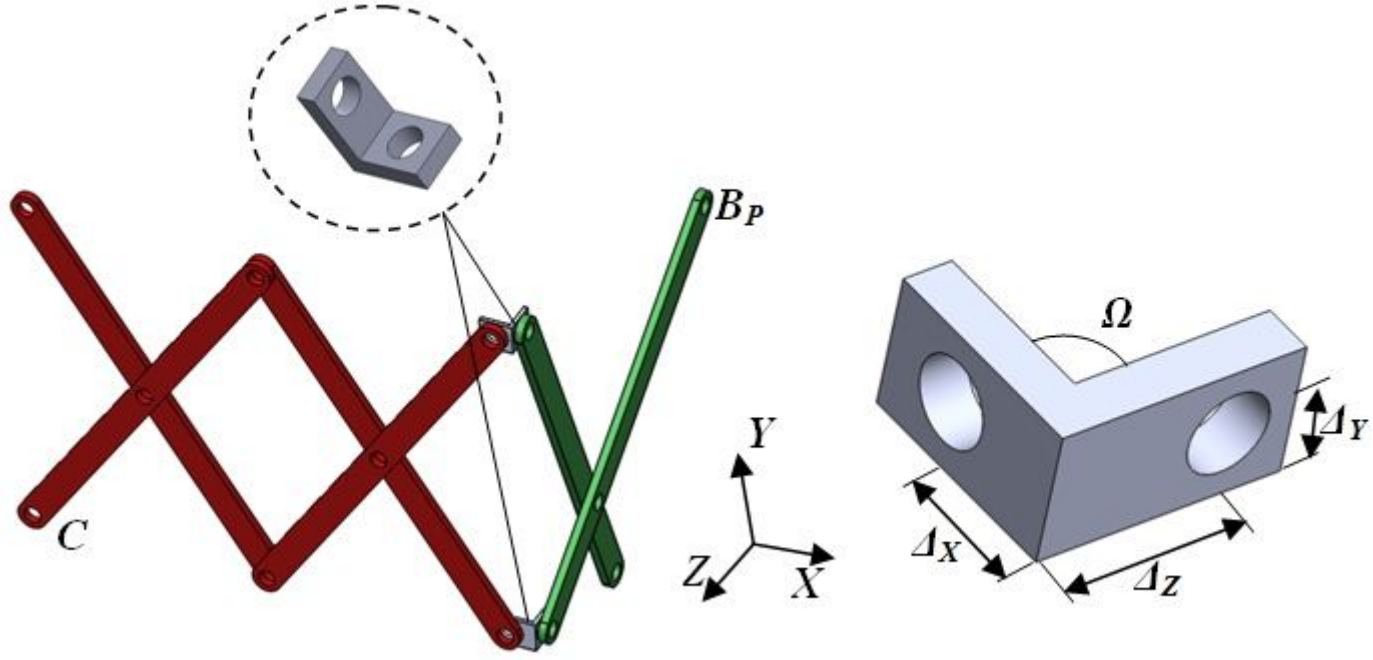

Figure 5

Connector. Description of its geometrical parameters.

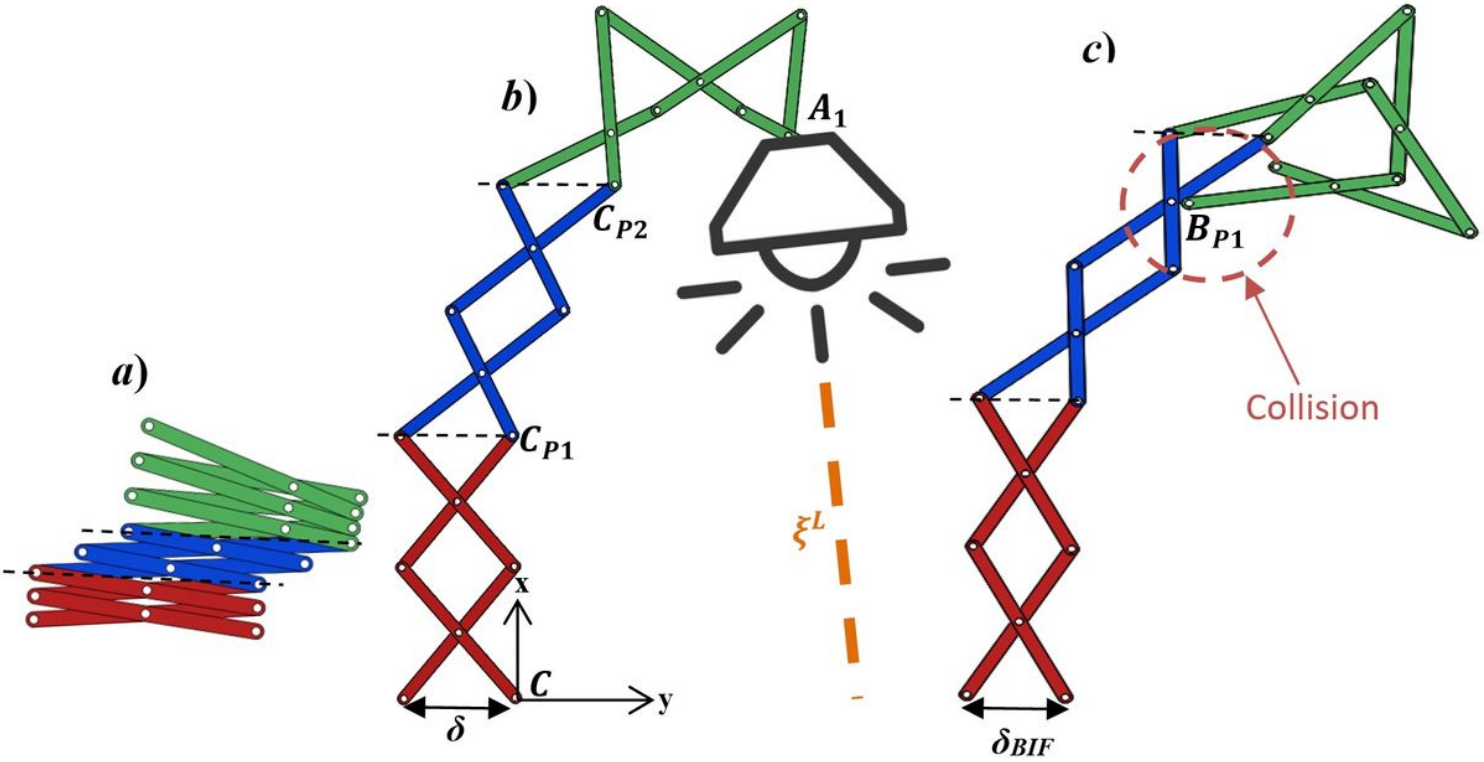

Figure 6

Retractable lamp. a. folding state b. intermediate position c. collision.

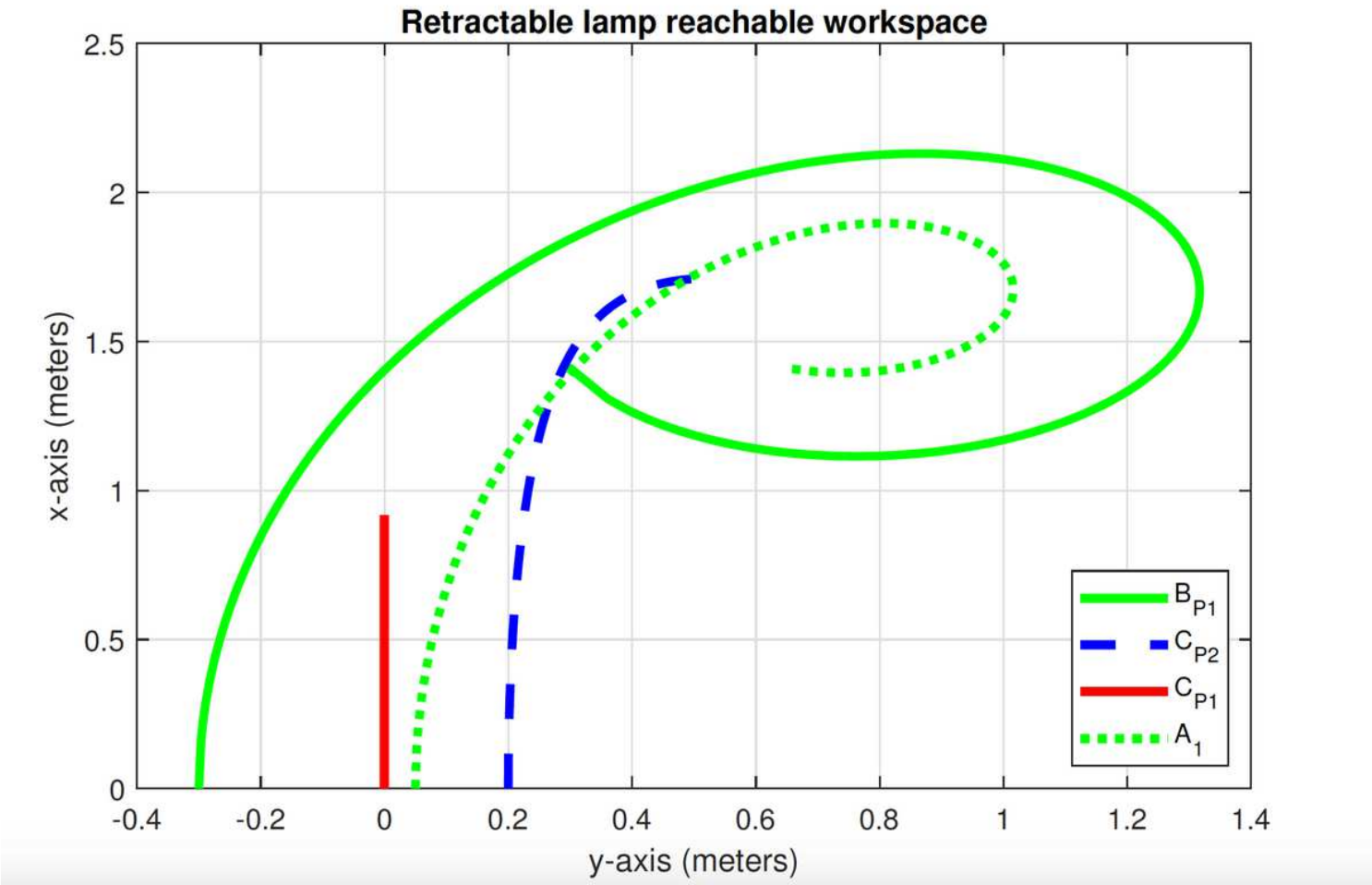

Figure 7

Workspace analysis. Reachable workspace of points A1, BP1, CP1, CP2.

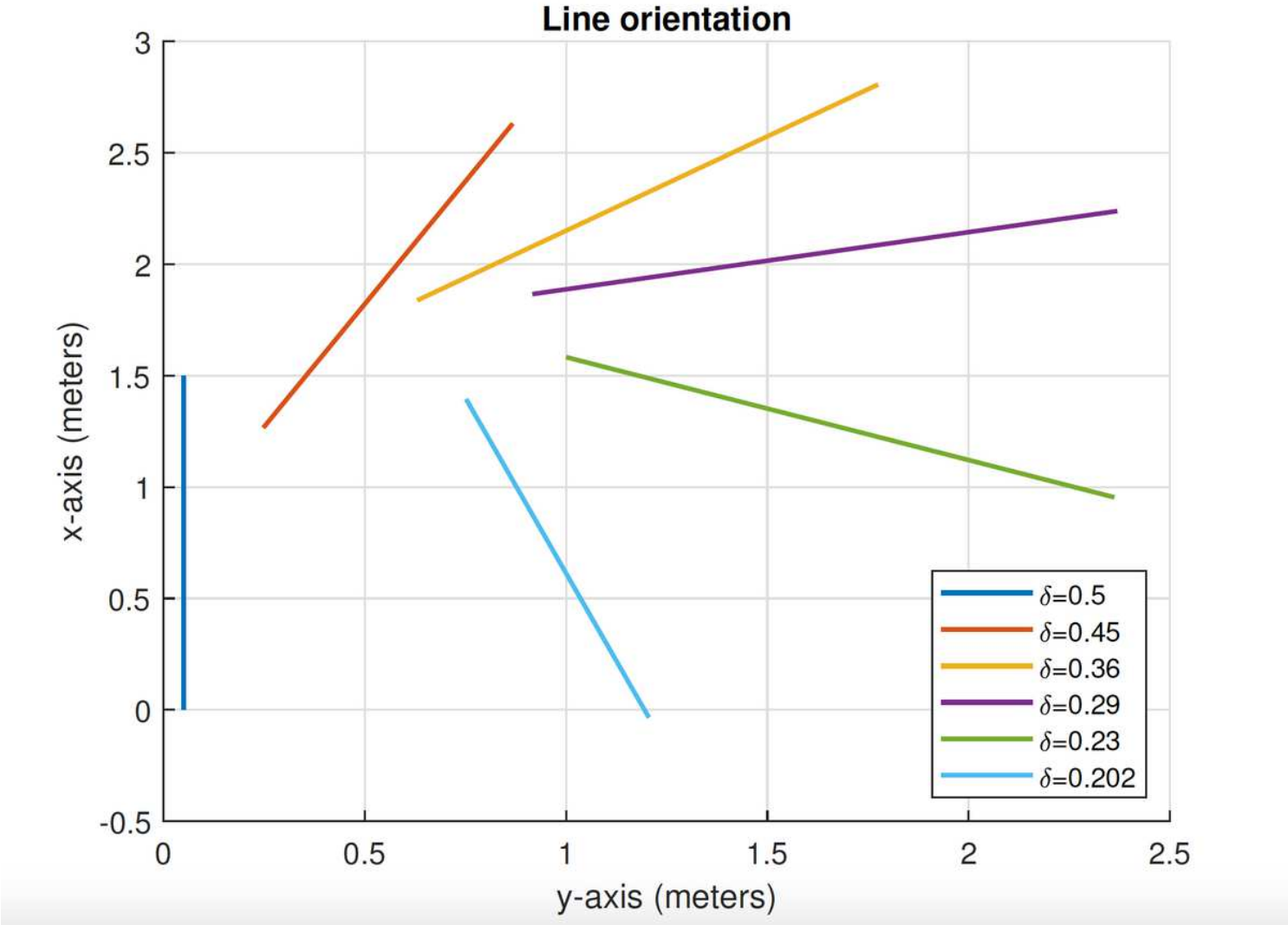

Figure 8

Light beam. Orientation of the light beam represented by a line on the x-y frame.

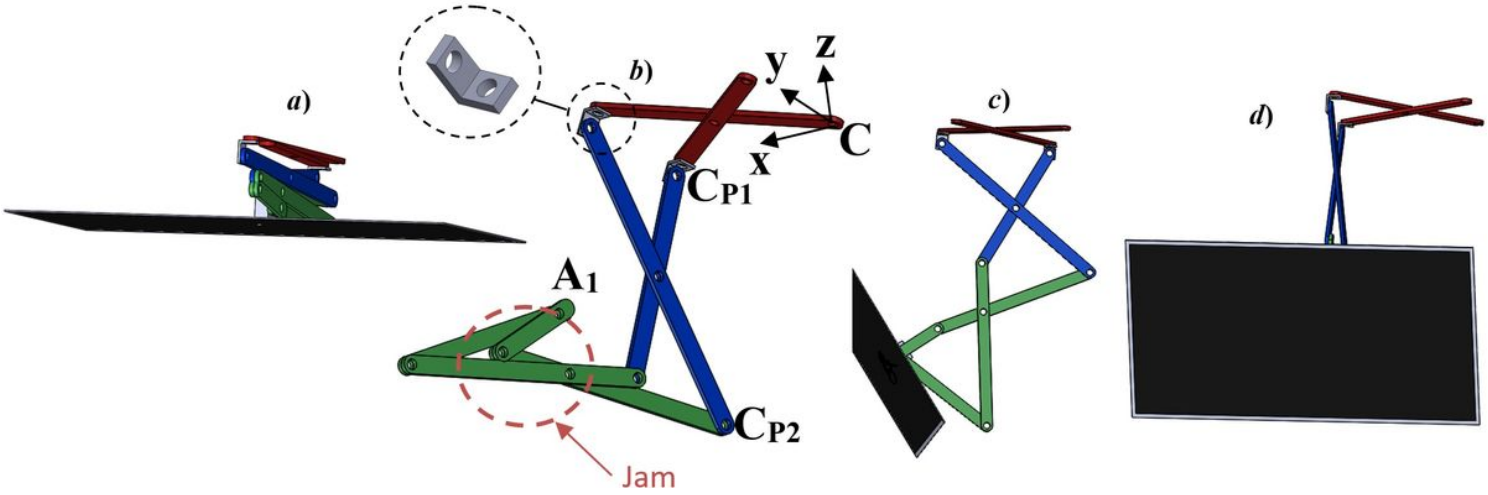

Figure 9

Folding furniture for flat displays. a. deploying condition b. singularity c. side view d. front view.

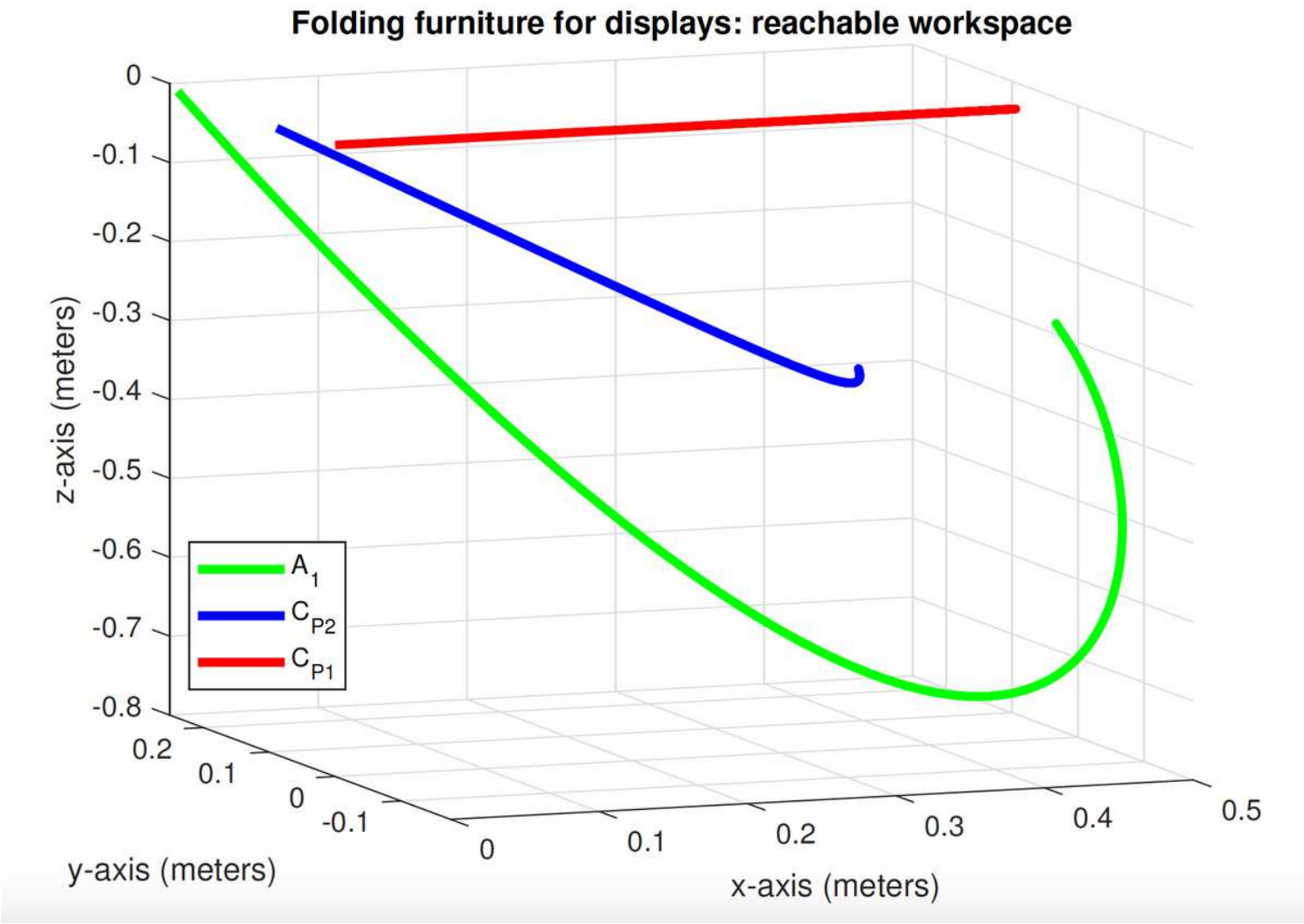

Figure 10

Workspace analysis. Reachable workspace: points A1, CP1, CP2.

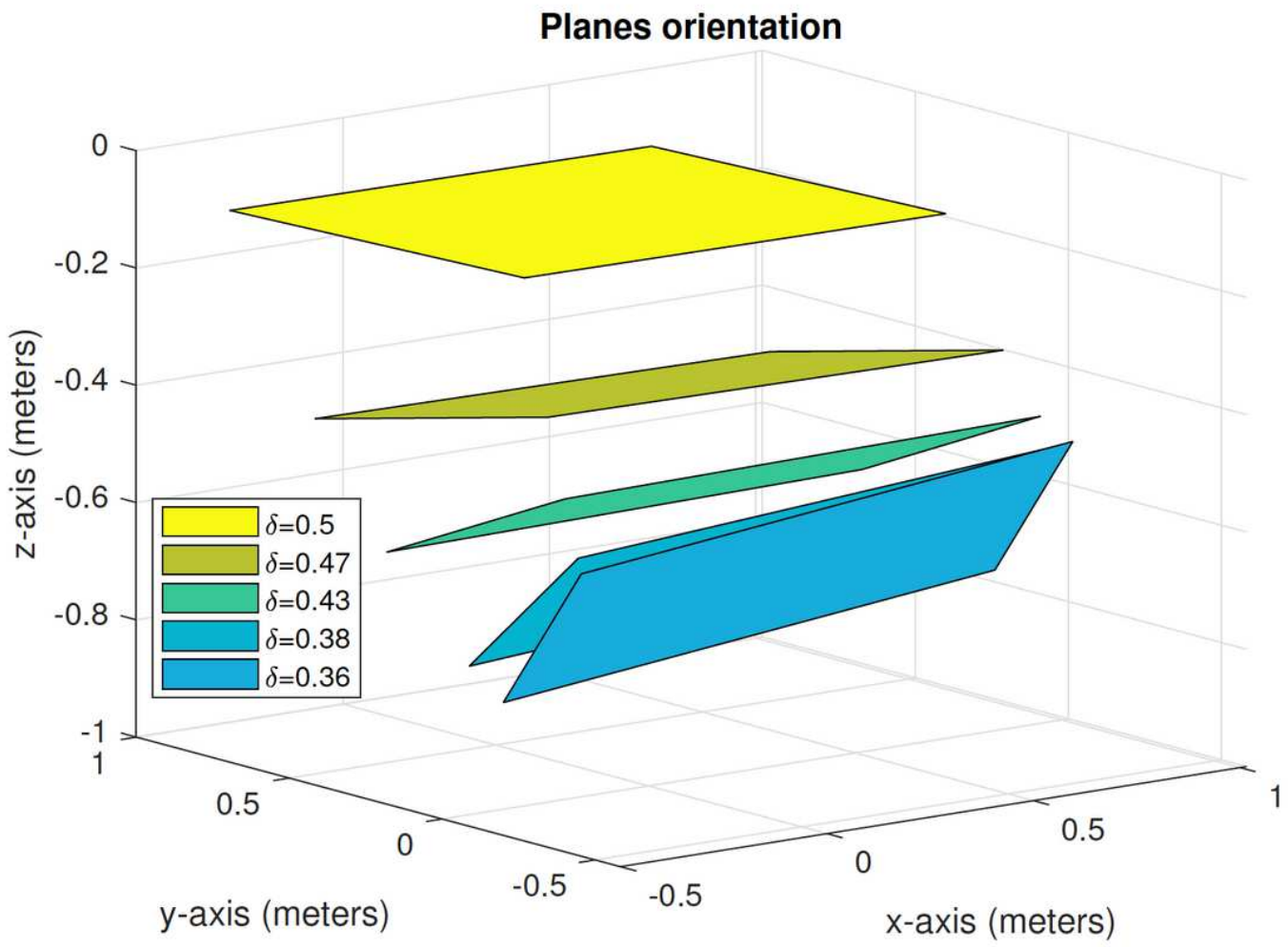

Figure 11

Folding furniture for TV. Orientation for planes emulating a at display.